치의학박사 학위논문

Metal–Ceramic Bond Strength and Mechanical Properties of Co–Cr Alloy Fabricated by Selective Laser Melting

선택적 레이저 용융 방식으로 제작한 코발트–크롬 합금의 금속–세라믹 결합강도와 기계적인 성질

2020년 8월

서울대학교 대학원
치의과학과 치과보철학 전공
홍 준 기

Metal–Ceramic Bond Strength and Mechanical Properties of Co–Cr Alloy Fabricated by Selective Laser Melting

지도교수 김성균

이 논문을 치의과학박사 학위논문으로 제출함

2020년 05월

서울대학교 대학원

치의과학과 치과보철학 전공

홍준기

홍준기의 박사 학위논문을 인준함

2020년 07월

위 원 장 ____________________ (인)

부위원장 ____________________ (인)

위 원 ____________________ (인)

위 원 ____________________ (인)

위 원 ____________________ (인)

-Abstract-

Metal–Ceramic Bond Strength and Mechanical Properties of Co–Cr Alloy Fabricated by Selective Laser Melting

Joon-Ki Hong, DDS, MSD

Department of Prosthodontics, Graduate School, Seoul National University

(Supervised by Professor ***Seong-Kyun Kim****, DDS, MSD, PhD)*

Purpose: The application range of 3D printing technology in the dental field is increasing due to the development of additive manufacturing technology and the advantages of manufacturing methods. However, there is a lack of research on differences in various characteristics when a prosthesis produced by 3D printing is compared with one produced by a conventional method. The purpose of this study is to determine whether there are differences in characteristics (metal-ceramic bond strength, mechanical properties) of metal depending on different manufacturing methods (casting, milling, and selective laser melting).

Materials and methods: To measure the mechanical properties of alloys, Co–Cr alloy specimens were prepared in three different ways: via casting using ingots (Star Loy C, Dentsply Sirona, Pennsylvania, USA), milling using milling disks (Starbond Co–Cr block, Scheftner

Dental Alloys, Mainz, Germany), or selective laser melting (SLM) using powder (SP2, EOS, Krailling, Germany). Specimens were fabricated in the shape of a 34 × 13 × 1.5 mm plate in accordance with ISO 22674:2016. Twelve specimens were prepared for each group. The flexural stress‑strain curves of the metals were drawn based on the results of three-point bending tests. Afterward, elastic modulus, yield strength, and flexural strength values were calculated. In addition, to measure their metal‑ceramic bond strength values, specimens were prepared in the same way as 25 × 3 × 0.5 mm plates in accordance with ISO 9693-1:2012. An 8 × 3 × 1.1 mm ceramic part (Hera Ceram, Heraeus, Hanau, Germany) was applied in the center portion above it. For each of the 12 specimens produced, the metal‑ceramic bond strength (τ_b) value was measured through three-point bending tests. After the experiment, five specimens were randomly selected from each group, and their surface roughness (R_a) values were measured at three sites per specimen. Next, the surface of specimens was analyzed via energy dispersive X-Ray spectroscopy (EDX) after the ceramic part had been removed. In addition, the surface where the metal had broken and the surface from which the ceramic part fell off were observed using scanning electron microscopy (SEM). The results of the tests were checked for equal dispersion by applying the Levene's test, and the influence of manufacturing methods on R_a, elastic modulus, yield strength, flexural strength, and metal‑ceramic bond strength values, as well as the percentage of ceramic remaining on the surface, were statistically analyzed using one-way ANOVA (analysis of variance) followed by

Tukey's Post-hoc test (α = 0.05).

Results: The R_a values were not statistically different (casting group 1.19 ± 0.58 μm, milling group 0.88 ± 0.46 μm, and SLM group 1.10 ± 0.30 μm), the elastic modulus value was the largest for the casting group (casting group 560.53 ± 21.53 GPa, milling group 473.55 ± 35.02 GPa, and SLM group 464.55 ± 10.77 GPa), and the yield strength value (casting group 567.92 ± 35.53 MPa, milling group 323.86 ± 32.04 MPa, and SLM group 591.18 ± 22.31 MPa) and the flexural strength value (casting group 792.31 ± 81.64 MPa, milling group 494.16 ± 51.93 MPa SLM group 849.48 ± 24.45 MPa) were the smallest for the milling group.

By observing the fracture surface of the metals via SEM, characteristic dendritic and inter-dendritic structures resulting from non-uniform cooling after casting were observed in the casting group, uniform surfaces were observed in the milling group, and the SLM group showed nanosized crystalline structures. Wave striations were observed on the fracture surface of the milling group, while the SLM group showed cleavage step patterns. The casting group attained a high τb value (casting group 32.51 ± 2.68 MPa, milling group 26.98 ± 3.97 MPa, and SLM group 29.07 ± 2.90 MPa). However, all three groups passed the ISO standard test.

Ceramic remains on the surface after removing the ceramic were observed. From the results of the component analysis using EDX, the proportion of silicon detected on the surface is in the order of the milling group, the SLM group, and the casting group, all of which showed a mixed failure pattern (casting group 36.44 ± 6.37%, milling group 57.10 ± 12.26%, and SLM group 49.50 ± 7.69%).

Conclusions: The R_a values of the Co‑Cr alloys produced by the three different methods were not different. Among the mechanical properties tested, the elastic modulus value was high for the casting group and yield strength and flexural strength values were low for the milling group. Every specimen showed a mixed failure pattern. Although there were differences in the results for the casting, milling, and SLM manufacturing methods, it was found that they all passed the test of bond strength according to the ISO standards. Considering many other advantages, the SLM method seems to have the potential to replace the traditional fabrication method.

Keyword: 3D printing; selective laser melting; Co‑Cr alloy; metal‑ceramic bond strength; three-point bending test
Student Number: 2017-36370

CONTENTS

I. INTRODUCTION

With the development of computer-aided design/computer-aided manufacturing (CAD/CAM) technology, CAD/CAM prostheses are frequently used in dental clinics.[1] In recent decades, metal-ceramic prostheses made of cobalt-chrome (Co-Cr) alloys have been used extensively.[2] Co-Cr alloy is one of the most widely used dental alloys due to its low price, high mechanical strength, and good corrosion resistance.[3]

The casting method, most commonly used when producing Co-Cr frameworks, is applied by producing and casting a wax pattern. This conventional method is labor-intensive, can cause errors in the manufacturing process, and is prone to human error.[4] However, recently, it has become possible to create Co-Cr frameworks via methods different from the traditional one owing to the development of CAD/CAM technology.[5]

Two of the new methods are milling and selective laser melting (SLM). These are less time-consuming and make mass production easier than the casting method. Co-Cr is an alloy that is often produced via CAD/CAM fabrication methods and is also frequently used when producing porcelain fused to metal (PFM) restoration.[6] In addition, Co-Cr alloy is used more often because it has the advantage of better biocompatibility than Ni-Cr alloy.[7,8]

The milling technique is a subtractive method that makes a metal structure by cutting a prefabricated metal disk. The milling method can eliminate defects or dimples in structures that can occur during casting since the disc used for milling can be manufactured in a highly standardized industrial environment.[9]

The SLM technique is an additive method in which fine structures are stacked while melting metal powder with a high-power laser beam. The SLM manufacturing method has several advantages. Complex structures can be produced with minimal wastage of material, reduced errors due to technicians making mistakes, and better quality products due to improved productivity. Moreover, production costs can be reduced through mass production. In addition, because it takes less time to manufacture, it can provide greater benefits to patients and clinicians.[10]

Before clinically using a material produced in a new way, it is necessary to ensure that its various properties are clinically appropriate. Such properties include biocompatibility, corrosion resistance, marginal fit, and mechanical properties. Although there are various mechanical properties, the yield strength and flexural strength are important factors because the metal should not fracture or deform when masticatory force is applied in the oral environment.

The most common clinical complication when using metal–ceramic prostheses is fracturing of the ceramic area.[11] Therefore, among the various properties, the metal–ceramic bond strength is important.[12] Despite the many advantages of the SLM method, there has been little research conducted on the metal properties and the bond strength with ceramics. Among the various test methods, the three-point bending test is widely used as the standard for measuring metal–ceramic bond strength and is also listed in the ISO regulations for dental restorations.[13,14]

The objective of this study is to examine how the Co‑Cr framework made by various methods differs in metal‑ceramic bond strength and its mechanical properties. The null hypothesis is that there is no difference in metal‑ceramic bond strength and mechanical properties according to the fabrication method of the Co‑Cr alloy.

II. MATERIALS AND METHODS

A flow chart of the entire experiment is shown in Figure 1. The Co‐Cr alloy was manufactured in three different ways after which mechanical properties test and metal‐ceramic bond strength tests were performed.

Preparation of Metal Specimens for Mechanical Properties Testing

To test the mechanical properties, metal specimens were fabricated by casting, milling, and SLM methods (n = 12 per group). The dimensions of the plate-shaped specimens according to ISO 22674:2016 are presented in Figure 2.

In the casting group, Co‐Cr specimens were made via the conventional lost-wax technique. Wax was cut into a plate-shaped dimension as a template and mounted in a casting ring. Samples were invested in a phosphate-bonded investment (Bc-vest Cb-formula, Bukwang, Seoul, Korea). Afterward, the rings were put into a furnace (Miditherm 100MP, BEGO, Bremen, Germany) for evaporation of wax. The casting was made using the Co‐Cr alloy ingots (Star Loy C, Dentsply Sirona, Pennsylvania, USA) in a casting device (Casting machine, Seki Dental, Seoul, Korea) according to the manufacturer's instructions. There was no post-production heat treatment after cooling at room temperature.

Milling group specimens were designed by CAD software

(3shape CAD, 3shape, Copenhagen, Denmark) and transferred to CAM software (HyperDENT, 3DBioCAD, Washington, USA). The specimens were milled from a prefabricated Co‐Cr alloy disk (Starbond Co‐Cr block, Scheftner Dental Alloys, Mainz, Germany) using a milling machine (Arum 5x-200, Arum, Frankfurt, Germany) according to the manufacturer's instructions. There was no post-production heat treatment of the milling group.

SLM group specimens were designed by CAD software (EOS RP Tools, EOS, Krailling, Germany) and transferred to CAM software (3shape Cambridge, 3shape). Subsequently, specimens were printed using a 3D-printer (EOSINT m270, EOS) with a 200 W Yb-fiber laser on the Co‐Cr powder (SP2, EOS) while building in the vertical direction. The manufacturing parameters were as per the manufacturer's instructions. The size of the Co‐Cr powder was 10‐45 μm, the building layer thickness was 20 μm, and the scan speed during the building process was up to 7.0 m/s. The heat treatment was applied in a muffle furnace (Muffle furnace 1000, Daeheung, Incheon, Korea) at 700 ℃ for 50 min.

After the fabrication of each group of specimens, the unnecessary parts of the metal surface were removed using stone points, and the surfaces were polished using rubber points. Afterward, the samples were sandblasted with 80 μm aluminum oxide (Al_2O_3) particles under 4 bar pressure for 5 sec, followed by cleaning with an ultrasonic cleaner. The compositions of the alloys used to fabricate the specimens are reported in Table 1.

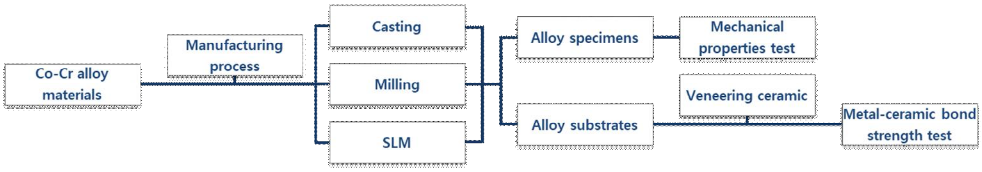

Figure 1. Overview flow-chart of the experiments.

Figure 2. Schematic diagram of the shape of the alloy specimens.

Table 1. Specification of the materials used in this study.

Group	Brand Name	Composition (wt%)	CTE ($\times 10^{-6} K^{-1}$)	Manufacturer
Casting	Star Loy C	Co 59.4%, Cr 24.5%, W 10%, Nb 2%, V 2%, Other(Mo, Si, Fe)≤ 1%	14.6 - 14.9	Dentsply Sirona, Pennsylvania, USA
Milling	Starbond Co - Cr block	Co 59%, Cr 25%, W 9.5%, Mo 3.5%, Other(Si, C, Fe, Mn, N) ≤1%	13.9 - 14.2	Scheftner dental alloys, Mainz, Germany
SLM	SP2	Co 62%, Cr 24%, Mo 5%, W 4%, Other(Si, Mn, Fe)≤ 2%	13.9 - 14.3	EOS, Krailling, Germany
Ceramic	Hera Ceram	Glass (silica) based ceramic	13.5 - 14.9	Heraeus, Hanau, Germany

The information is provided by the manufacturer. CTE, coefficient of thermal expansion.

Surface Characterization

Five random specimens were selected per group, and the average surface roughness (R_a) of the base metal was determined using a confocal laser microscope (Zeiss LSM 800 MAT & Zeiss Axio imager Z2m, Zeiss, Jena, Germany) with ZEN software (Zeiss). Imaging was performed using laser excitation at 405 nm with 20 × 0.7 NA over evaluation lengths of 319 μm. The tests were performed at different points on each specimen.

Preparation of the Metal‑Ceramic Specimens for Bond Strength Testing

The metal parts of the metal‑ceramic specimens were fabricated using the same devices and process (n =12 for each group). The dimensions of the substrates were 25 × 3.0 × 0.5 mm, which is in accordance with ISO 9693-1:2012. After polishing, sandblasting, and cleaning, a layer of an opaque ceramic (Hera Ceram PO A2) was applied, and a body ceramic (Hera Ceram D A2) was fused to the central areas (8 × 3 × 1.1 mm) of the metal bars (Figure 3). The firing procedure was performed in a Programat p500 furnace (Ivoclar Vivadent, Schaan, Liechtenstein) according to the manufacturer's instructions. Table 2 reports the firing schedules for the ceramic.

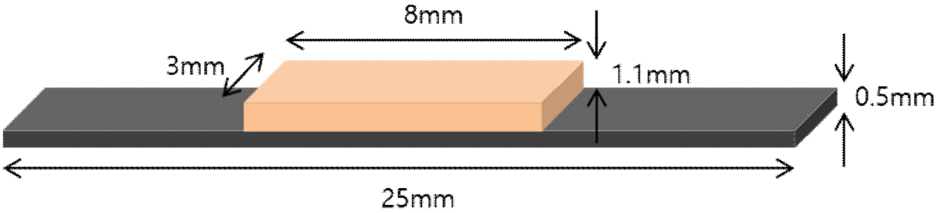

Figure 3. Schematic diagram of the shape of the metal-ceramic specimens. The orange part represents veneering ceramic and the black part represents metal substrate.

Table 2. Firing schedules for the ceramic veneering procedure.

Product Name	Pre-heating Temp.(℃)	Drying Time (min)	Heating Rate (℃/min)	Final Temp.(℃)	Holding Time (sec)	Vacuum
Degassing	500	1	50	980	50	+
1st opaque	500	10	50	960	50	+
2nd opaque	500	10	50	950	50	+
Dentin	500	5	50	930	38	+
Glaze	500	2	50	901	38	+

Mechanical Properties Testing and Microstructure Analysis

Three-point bending tests were performed on the metal specimens according to ISO 22674:2016 using a universal testing machine (Instron 8871, Instron, Massachusetts, USA); the crosshead speed was 1.5 mm/min until the specimen fractured. The distance between the supports was 20 mm and the radius of the bending piston was 2 mm (Figure 4.).

The 0.2% yield strength and flexural strength were calculated from the recorded load and crosshead movement. Flexural stress and flexural strain were computed as

$$Flexural\,stress\,\sigma_f = \frac{3FL}{2bd^2}$$
$$Flexural\,strain\,\epsilon_f = \frac{6Dd}{L^2}$$

where F is the load at a given point on the load-deflection curve (N), L is the support span (mm), b is the width of the test beam (mm), d is the depth or thickness of the test beam (mm), and D is the maximum deflection of the center of the beam (mm).

After the three-point bending tests, the fractured surface and the original unbroken surface were subjected to scanning electron microscopy (SEM; AURIGA, Zeiss, Oberkochen, Germany) on secondary electron mode and backscattered electron (BSE) mode to observe fracture patterns and microcrystalline structures.

Metal - Ceramic Bond Strength Testing

The metal - ceramic specimens were tested in a universal testing machine (TW-D102, Taewon Tech., Seoul, Korea). According to ISO 9693-1:2012, the distance between the supports was 20 mm and the radius of bending piston was 1 mm. The specimen was placed at the center and the crosshead speed of the loading part was 1.5 mm/min (Figure 5). The tests were run until debonding/cracking commenced. The bond strength (τ_b) was calculated as follows:

$$\tau_b = F_{fail}(A \times d_m^2 + B \times d_m + C)$$

where A, B, and C are correction factors calculated using the elastic modulus of the three-point bending test and d_m is the thickness of the specimen (mm).

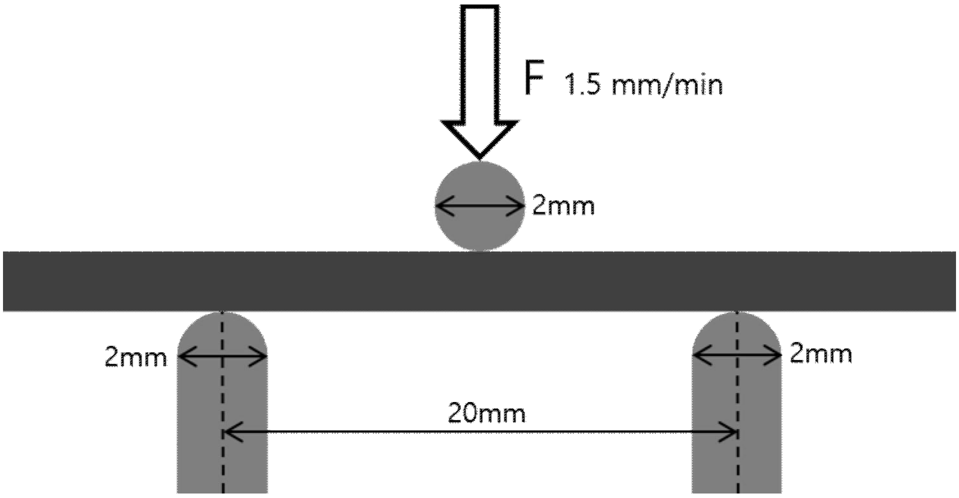

Figure 4. Schematic diagram showing the three-point bending test for the mechanical properties. The distance between the supports was 20 mm and the radii of the bending piston and supports were 2 mm. The bending piston was placed at the center and crosshead speed of the loading part was 1.5 mm/min.

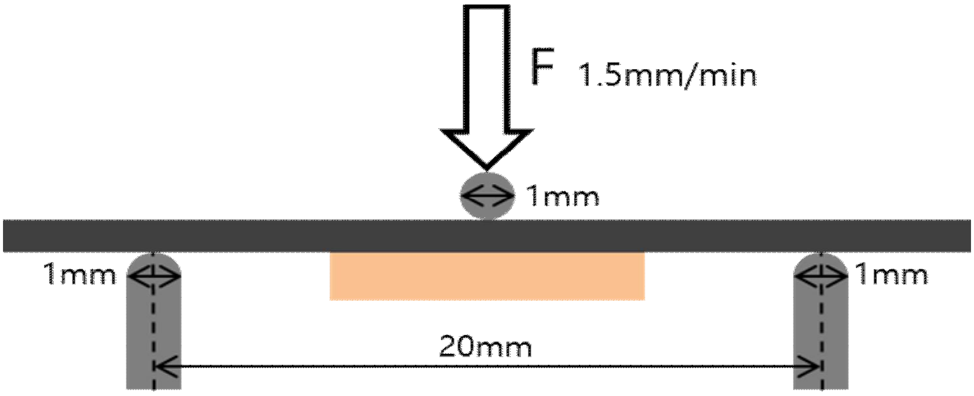

Figure 5. Schematic diagram showing the three-point bending tests to measure the metal-ceramic bond strength. The distance between the supports is 20 mm and the radii of the bending piston and supports were 1 mm. The bending piston was placed at the center and crosshead speed of the loading part was 1.5 mm/min.

Fracture Mode Analysis

After the metal‐ceramic bond strength test, fracture sites were examined via SEM. Five random specimens from each group were selected, and specimens were disassembled manually to analyze the fractured surface. The metal‐ceramic interface was observed by the naked eye, and the images were taken using a digital camera. Subsequently, the fractured surface was analyzed via SEM and energy dispersive X-Ray spectroscopy (EDX) to detect the distribution of Si remaining on the surface. EDX imaging was performed under 170 × magnification on an evaluation area of 1650 × 1200 μm at 3 different areas on each specimen.

The failure mode was classified into three types: adhesive (less than 20% of the alloy surface covered by the remaining ceramic), mixed (20‐80%), and cohesive (> 80%) by analyzing the data of Si detection with software (ImageJ, NIH, MD, USA).

Statistical Analysis

IBM SPSS Statistics Version 22 (IBM, Armonk, New York, USA) was used for statistical analysis. Levene's test was applied to assess the equality of the variances. The data on roughness, elastic modulus, 0.2% yield strength, flexural strength, bond strength, the ratio of Si remaining on the surface were analyzed using one-way ANOVA (analysis of variance), followed by Tukey‘s Post-hoc test ($\alpha = 0.05$).

III. RESULTS

Surface Roughness of the Metal Substrate

The R_a values for each group are reported in Table 3. The casting group had the highest R_a value, followed by the SLM group and the milling group. However, there were no statistically significant differences between the three groups ($p > 0.05$).

Table 3. Surface roughness values of the test groups.

Group	R_a(μm)
Casting	1.19±0.58
Milling	0.88±0.46
SLM	1.10±0.30

The results are expressed as the mean ± standard deviation. R_a, surface roughness.

Mechanical Properties of the Co‐Cr Alloy

Table 4 and Figure 6 summarize the mechanical properties of the Co‐Cr alloys of each group calculated through measurements, while Figure 7 shows the stress‐strain curve of each group. The elastic modulus value was higher in the casting group (Figure 6A; $p < 0.05$). Differences in the yield strength and flexural strength values between the casting and SLM groups were not statistically significant but were lower in the milling group (Figure 6B and 6C; $p < 0.05$).

The casting and SLM groups satisfied the minimum required elastic modulus values (150 GPa) and yield strength values (500 MPa) for class 5 of ISO 22674:2016 (class 0: small veneered one-surface inlays, veneered crowns; class 1: veneered or un-veneered one-surface inlays, veneered crowns; class 2: crowns or inlays without restriction on the number of surfaces; class 3: multiple-unit fixed prostheses; class 4: removable partial dentures, clasps, thin veneered single crowns, and full-arch fixed dental prostheses; and class 5: thin removable partial dentures, parts with thin cross-section, clasps), but the milling group showed low yield strength (270 - 360 MPa), so it can only be used for classes 0 to 3.

Table 4. Mechanical properties of the specimens.

Group	Elastic Modulus (GPa)	0.2% Yield Strength (MPa)	Flexural Strength (MPa)
Casting	560.53±21.53*	567.92±35.53	792.31±81.64
Milling	473.55±35.02	323.86±32.04*	494.16±51.93*
SLM	464.55±10.77	591.18±22.31	849.48±24.45

The results are expressed as the mean ± standard deviation. *, Statistically significantly different compared to the other groups ($p < 0.05$).

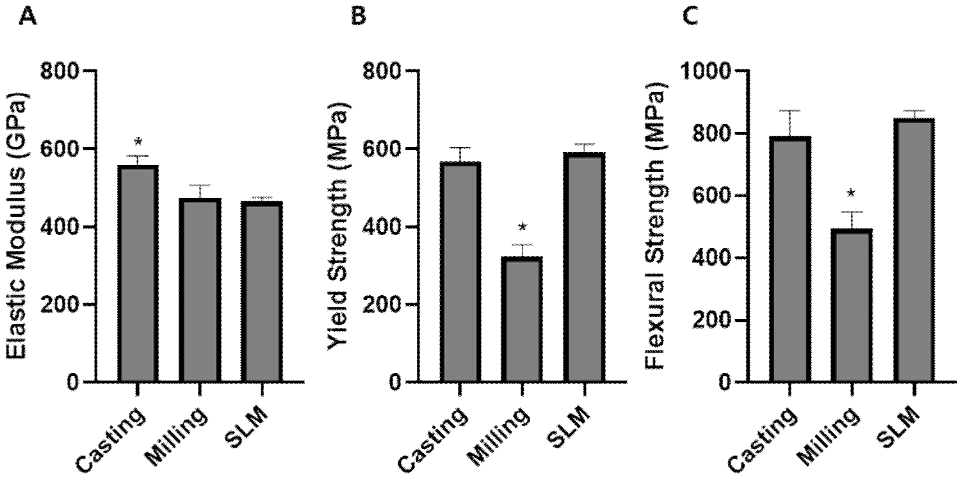

Figure 6. Mechanical properties of the casting, milling, and SLM groups: (A) elastic modulus, (B) yield strength, and (C) flexural strength. *, statistically significantly different compared to the other groups ($p < 0.05$).

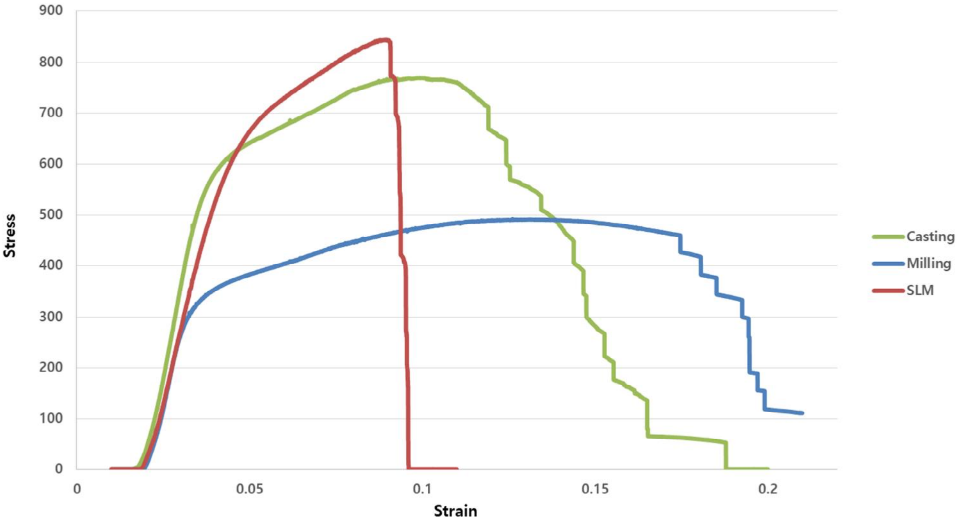

Figure 7. Mean stress‐strain curves from the three-point bending test results. The casting group (green line) showed high elastic modulus, while the milling group (blue line) showed low yield strength and flexural strength.

Microstructure of the Co - Cr Alloy

Figure 8 shows the original unbroken smooth surface of the Co - Cr specimens, while Figures 9 and 10 show SEM images of the fractured Co - Cr specimens. The images in Figures 8 and 9 were taken in backscattered electron (BSE) mode. The casting group displayed typical inhomogeneous dendritic and inter-dendritic solidification microstructures (Figures 8A, 9A, and 10A). The grain size was approximately 50 - 100 μm. On the other hand, large crystalline structures were not evident in the milling group specimens (Figure 8B) and showed homogeneous surfaces. For the SLM group, nanosized crystalline structures can be seen in Figure 8C, while a layered structure was observed at the fractured surface (Figures 9E and 10C).

In the fractured surface of the casting group, it can be observed that the fracture occurred along the dendritic structure. On the fracture surface of the milling group, a wave pattern of striations can be observed on the surface (Figures 8D and 9B), which means that the specimen was stretched and fractured, implying that the material has good ductility. Stair-like cleavage steps are evident on the fractured surface of the SLM group (Figures 8E and 9C), which is usually seen with brittle materials.

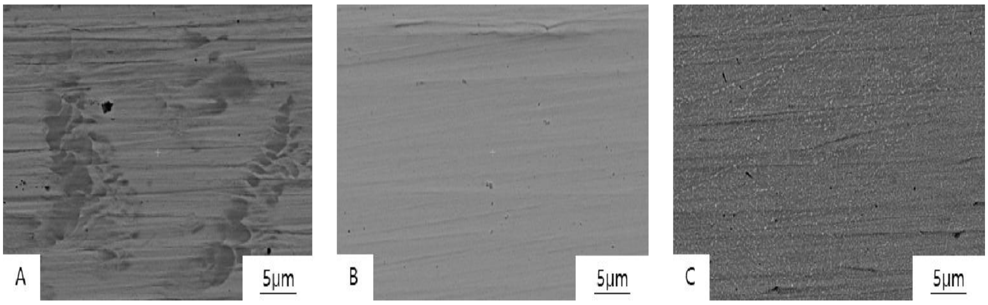

Figure 8. BSE images of the original unbroken surfaces of Co-Cr alloy specimens: (A) casting (10000 ×; the dark shaded areas indicate dendritic crystal structures), (B) milling (10000 ×; a uniform surface can be observed), and (C) SLM (10000 ×; small crystalline structures that look like white grains can be observed).

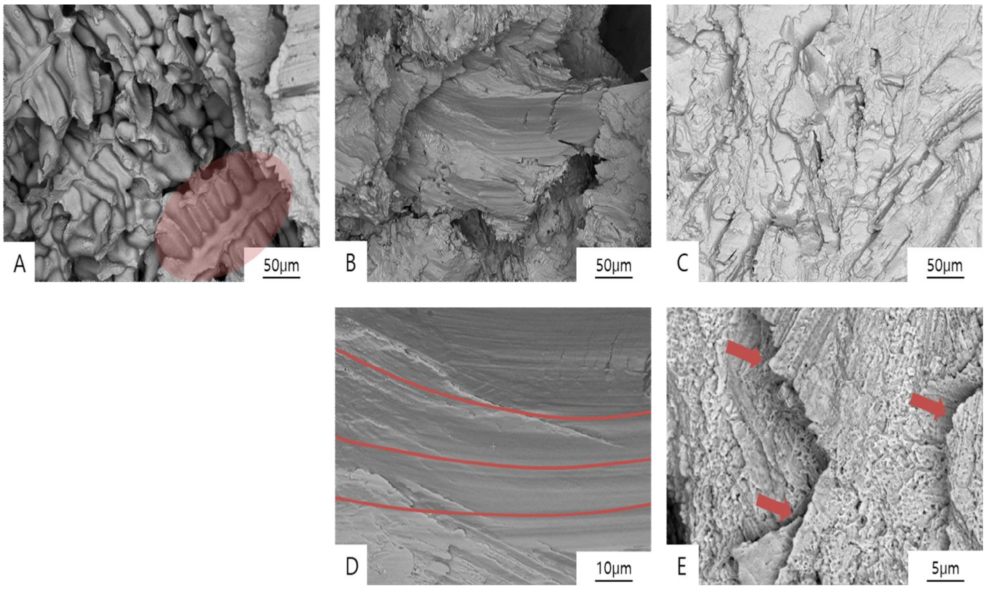

Figure 9. BSE images of the fractured surface of the Co-Cr alloy specimens: (A) casting (1000 ×; the red oval shading indicates a dendritic structure), (B) milling (1000 ×), (C) SLM, (1000 ×), (D) milling (5000 ×; the red lines signify striations), and (E) SLM (10000 ×; the red arrows indicate cleavage steps).

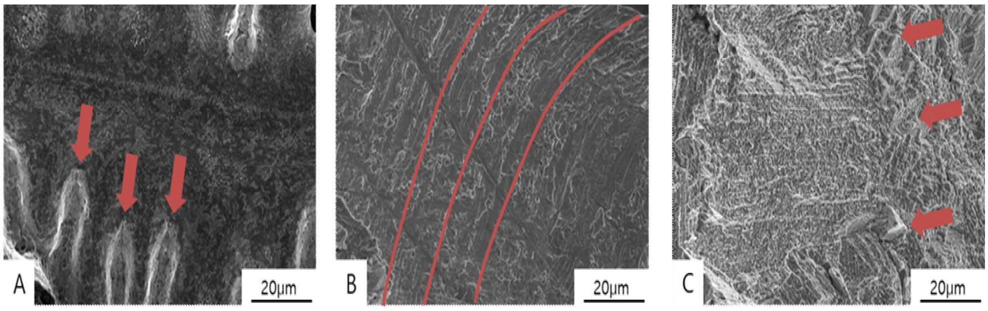

Figure 10. SEM images of the fractured surface of the Co-Cr alloy specimens: (A) casting (4000 ×; the red arrows indicate dendritic structures, (B) milling (4000 ×; the red lines signify striations), and (C) SLM (4000 ×; the red arrows indicate cleavage steps).

Metal - Ceramic Bond Strength of the Co - Cr Alloy

Table 5 and Figure 11 present the results of the metal-ceramic bond strength experiments. The casting group showed the highest value ($p < 0.05$), while there was no significant difference between the other two groups. According to ISO 9393-1: 2012, at least four out of six specimens must have bond strength ≥ 25MPa to pass the test. Therefore, all three groups passed the test.

Table 5. Metal-ceramic bond strength and passing rate (≥ 25MPa) of the specimens.

Group	Bond Strength (Mpa)	Passing Rate
Casting	32.51±2.68*	100.00%
Milling	26.98±3.97	66.67%
SLM	29.07±2.90	91.67%

The results are expressed as the mean ± standard deviation.

*, Statistically significantly different compared to the other groups ($p < 0.05$).

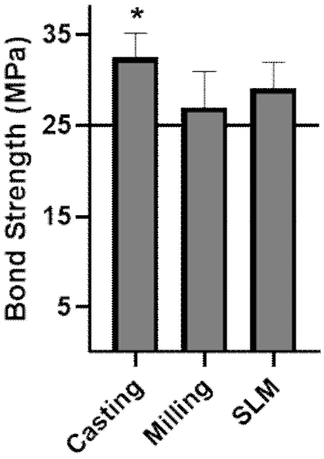

Figure 11. Metal-ceramic bond strength of the casting, milling, and SLM groups. The horizontal line at 25 MPa is the pass strength according to ISO 9693-1:2012.

*, statistically significantly different compared to the other groups ($p < 0.05$).

Observations of the Metal - Ceramic Failure Surfaces

Figure 12 shows the surface of the metals after ceramic debonding. In all three groups, it can be observed that the ceramic remained irregularly on the surface of the metal.

The ceramic was removed from the metal after the three-point bending test, and the metal specimens were placed and observed with a digital camera and SEM. The lower part is metal, and ceramic remains on the metal surface. In the casting group, small defects can be seen on the metal surface in Figure 13.

EDX Analysis

Figure 14 shows the Co - Cr surface after manually separating the ceramic layer. The EDX analysis of the light spot (spot 1) on the electron microscope image produced a high peak for Si whereas that of the dark spot (spot 2) produced a high peak for Cr.

After performing the three-point bending tests, the ratio of the area where Si was detected was calculated through EDX mapping to determine the proportion of ceramic remaining on the surface.

Table 6 shows the proportion of the surface on which Si was detected. A ratio of 20% or less indicates adhesive failure whereas 80% or more indicates cohesive failure. Ratios between 20 and 80% are regarded as mixed failure. From the results of the analysis, the ratio increased in the order of casting, SLM, and milling. All specimens showed mixed failure patterns.

Table 6. Failure mode analysis results and the area fraction of Si detected.

Group	Area fraction of Si detected (%)	Failure mode
Casting	36.44±6.37^{a}	Mixed
Milling	57.10±12.26^{b}	Mixed
SLM	49.50±7.69^{a,b}	Mixed

The results are expressed as the mean ± standard deviation. Different lowercase letters indicate a significant difference between groups ($p < 0.05$).

Figure 12. Metal-ceramic failure surface after debonding of the ceramic: (A) casting, (B) milling, and (C) SLM

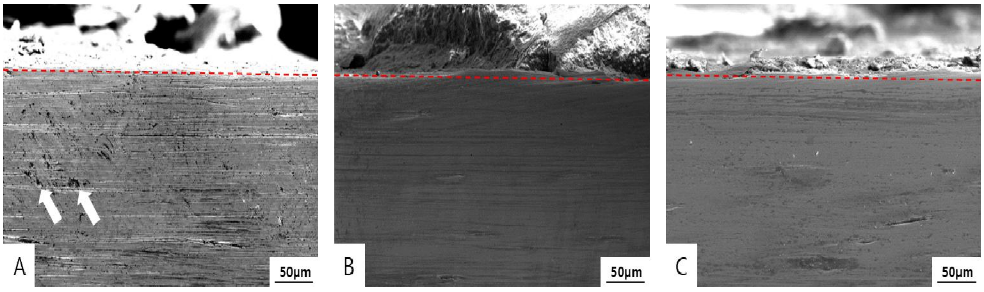

Figure 13. Horizontal SEM image of the metal-ceramic specimen after debonding of the ceramic: (A) casting (the white arrows indicate defects), (B) milling, and (C) SLM. The red dotted lines indicate the metal-ceramic boundaries.

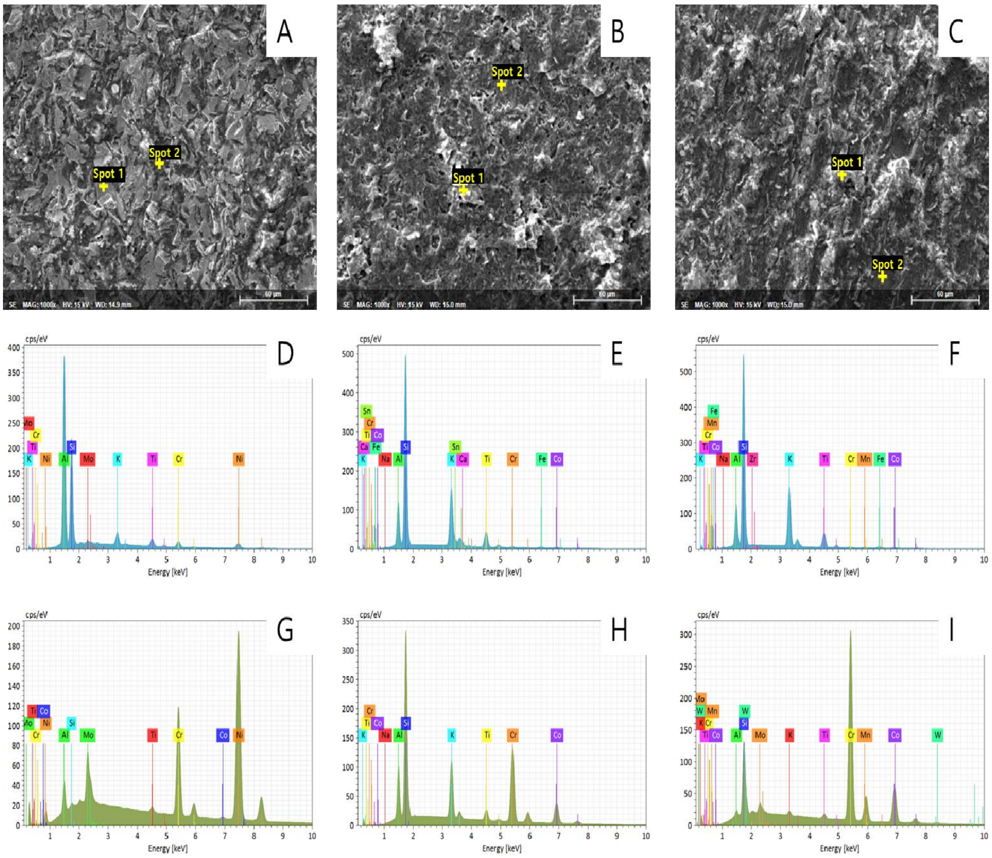

Figure 14. SEM images (1000 ×) of a (A) casting, (B) milling, and (C) SLM specimens. EDX analysis of the Co‑Cr alloy surface after removal of the ceramic layer: spot 1 of the (D) casting, (E) milling, and (F) SLM specimens showing a high peak for Si and spot 2 of the (G) casting, (H) milling, and (I) SLM specimens showing a high peak for Cr.

IV. DISCUSSION

In this study, the properties of Co‐Cr alloys made via different methods were investigated. The mechanical properties and metal‐ceramic bond strength of the alloys varied depending on the manufacturing method. Summing up the experimental results, the null hypothesis that the method of manufacturing the alloy does not affect the properties of the metal was rejected.

Measuring the mechanical properties of alloys is very complex. Different standards and methods are used to measure the needs of each field and situation.[15-18] For instance, the commonly used standard for measuring the mechanical properties of alloys used in dental prostheses is ISO 22674:2016.[19]

From the results of examining the mechanical properties in this experiment (Table 4 and Figure 6), the casting group showed the highest elastic modulus. A higher elastic modulus value means that more stress is required when the alloy is deformed by the same amount. The milling group showed the lowest yield strength and flexural strength. Lower yield strength means that plastic deformation occurs at lower stress levels, while lower flexural strength means that flexion fracturing occurs at lower stress levels. Zhou et al.[20] tested the mechanical properties of SLM, milling, and casting Co‐Cr alloys and found that the SLM group showed higher yield strength, tensile strength, and elongation. Kim et al.[21] also tested the mechanical properties of SLM, milling/post-sintering, milling and casting Co‐Cr alloy, and reported that the milling group specimens were inferior to those of the other groups. Jabbari et al.[22] found higher hardness values in their SLM group than in their casting group.

According to the stress‐strain curves in Figure 7, the toughness, the total energy absorbed until fracturing was higher in the casting group. In the SLM group, fracturing occurred at a low strain level, and so it can be considered the most brittle. Øilo et al.[23] also tested 3-unit Co‐Cr alloy bridges and showed that the SLM frameworks were brittle and harder than the casting and milling specimens. The most deformation until fracturing occurred in the milling group, and so it is relatively ductile, whereas the SLM group is relatively brittle due to the fracturing under less deformation.

In the SLM manufacturing method, factors such as building direction, layer thickness, scan speed, and post-build heat treatment can affect the properties of the final product. In this study, a 200 W Yb-fiber laser was used to build in a vertical direction with a layer thickness of 20 µm and a scan speed of 7 m/s. Takaichi et al.[24] revealed that the yield strength in the tensile tests is dependent on the sample's building direction and that yield strength is higher in vertical direction printing than in height direction printing. Lu et al.[25] considered that a speed of 7 m/s with a laser power of 95 W, a track width of 0.11 mm, and a layer thickness of 25 µm are promising settings in terms of yield strength, corrosion resistance, and margin-fit accuracy. Moreover, Yan et al.[26] revealed that the post-building heat treatment of Co‐Cr alloy during the SLM method is effective for releasing residual stress, thereby leading to a homogenized microstructure and improving toughness.

According to the results of this study, the mechanical properties of alloys varied according to the fabrication method with the casting and SLM group specimens showing better values than those required by the standards in ISO 22674:2016. Although the yield strength and flexural strength of the milling group were the lowest, they are still suitable for use in class 3 (multiple-unit fixed prostheses) items.

From the measurements of metal‐ceramic bond strength, that of the casting group was the highest ($p < 0.05$, Table 5), which means that it was more difficult to separate the ceramic and metal parts. The reason for the difference in bond strength in each group can be explained by the differences in elastic modulus, chemical bonding, mechanical interlocking, and compressive bonding values.

The results of other studies in which the metal‐ceramic bond strength values of Co‐Cr alloys made by various fabrication methods were measured were similar to the present study in some cases and different in others. When comparing metal‐ceramic bond strengths of alloys produced by SLM and casting, Xiang et al.[27] and Wang et al.[28] reported higher bond strengths in the SLM group. On the other hand, Kaleli et al.[29], Li et al.[30], and Wu et al.[31] found that there were no statistically significant differences in bond strength between the casting, milling, and SLM groups. In addition, there was a study[32] showed that the milling group with high metal‐ceramic bond strength and the casting group with low bond strength.

In general, alloys with a high modulus of elasticity are more resistant to bending and peeling, which results in stronger metal-ceramic bond strength. Looking at the formula for obtaining bond strength,

$$\tau_b = F_{fail}(A \times d_m^2 + B \times d_m + C)$$

Since the bond strength is obtained through the failure force (F_{fail}) and constants A, B, and C, it is likely that the high elastic modulus could have caused the high bond strength of the casting group. In addition, ceramics are brittle and vulnerable to deformation, and when combined with a metal having a low elastic modulus, ceramic fracturing can easily occur due to a large amount of elastic deformation of the metal, even at low forces.

Chemical bonding occurs by chemisorption due to diffusion at the metal-ceramic interface and is affected by the oxide layer on the metal-ceramic interface.[33] Xin et al.[34] found that a thicker oxide layer was formed on the surface of the Co-Cr alloy produced by the SLM method than by casting, which can affect the chemical bonding at the metal-ceramic interface. How the thickness of the oxide layer varies depending on the method of manufacturing the metal and how it affects the metal-ceramic bond strength is an area requiring further study.

Mechanical interlocking is another factor influencing bond strength. In general, high roughness is known to help increase metal-ceramic bond strength.[35,36] It was found that the R_a values of the Co-Cr alloy surfaces measured in this study were not significantly different. However, this may not be the case when the surface properties are the same but the standard deviation is large. Therefore, further research to determine the effects of the alloy surface is required.

Compressive bonding is also one of the factors affecting metal - ceramic bond strength. When the coefficient of thermal expansion (CTE) value of the metal is slightly higher than that of the ceramic, it is called a positive mismatch. This causes the formation of strong metal - ceramic bonds during the cooling process after ceramic firing. Looking at the CTE values of the materials used in this study (Table 1), it can be seen that the CTE value of the casting ingot is higher than that of the ceramic whereas the materials used for milling and SLM had similar CTE values to the ceramic. This difference would have contributed to the higher bond strength of the casting group.

In this study, only the manufacture of the SLM-produced alloy specimens ended with a heat-treatment process. According to Yan et al.[37], when the heat treatment of the Co - Cr alloy produced via the SLM method was 880 or 1100 ℃, there was no difference in bond strength, while Xin et al.[38] reported that the ceramic firing process did not change the surface structure of the SLM alloy.

There is a method of treating the metal surface to increase the metal - ceramic bond strength. Dimitriadis et al.[39] reported a slight decrease in bond strength when a bonding agent was used on the surface of a Co - Cr alloy produced by SLM. Furthermore, Al Bakkar et al.[40] reported that the bonding agent on the Co - Cr surface had a minor effect on bond strength. Sandblasting of the alloy surface can also affect bond strength. Park et al.[41] reported that the acid-etching and sandblasting of the surface of Co‐Cr alloy help to increase the bond strength, while Külünk et al.[42] reported that sandblasting with 110-μm Al_2O_3 had a better effect on bond strength than with 50-μm Al_2O_3. In this study, samples were sandblasted with 80-μm Al_2O_3 particles, and a bonding agent was not used.

When the results of this study are put together, the SLM method satisfies the ISO 22674:2016 and ISO 9693-1:2012 standards for manufacturing dental prostheses. It is considered to be a suitable method for fabricating Co‐Cr alloys for clinical use because the product exhibits mechanical properties and metal‐ceramic bond strength values beyond the required standard values and the manufacturing method has several advantages, such as good productivity and reduced human error.

V. CONCLUSIONS

Within the limitation of this study, the following conclusions can be drawn. The mechanical properties of Co-Cr alloy depend on the manufacturing technique. The casing group specimens showed high elastic modulus values, while the milling group showed low yield strength and flexural strength values. All three groups exceeded the ISO standards for metal‑ceramic bond strength. According to ISO 22674:2016 and ISO 9693-1:2012, the SLM technique can be used for manufacturing dental prostheses. Considering many other advantages, the SLM method seems to have the potential to replace the traditional fabrication method.

REFERENCES

1 Bayne S, Heymann H. CAD/CAM in dentistry: present and future applications. Quintessence International. 1996;27:431-3.

2 Wataha JC. Alloys for prosthodontic restorations. Journal of Prosthetic Dentistry. 2002;87:351-63.

3 Roberts HW, Berzins DW, Moore BK, Charlton DG. Metal ceramic alloys in dentistry: a review. Journal of Prosthodontics: Implant, Esthetic and Reconstructive Dentistry. 2009;18:188-94.

4 Van Noort R. The future of dental devices is digital. Dental Materials. 2012;28:3-12.

5 Rekow E. A review of the developments in dental CAD/CAM systems. Current Opinion in Dentistry. 1992;2:25-33.

6 Miyazaki T, Hotta Y, Kunii J, Kuriyama S, Tamaki Y. A review of dental CAD/CAM: current status and future perspectives from 20 years of experience. Dental Materials Journal. 2009;28:44-56.

7 Geis-Gerstorfer J, Sauer K-H, Pässler K. Ion release from Ni-Cr-Mo and Co-Cr-Mo casting alloys. International Journal of Prosthodontics. 1991;4.2.

8 Wataha JC. Biocompatibility of dental casting alloys: a review. The Journal of Prosthetic Dentistry. 2000;83:223-34.

9 Strub JR, Rekow ED, Witkowski S. Computer-aided design and fabrication of dental restorations: current systems and future possibilities. The Journal of the American Dental Association. 2006;137:1289-96.

10 Mumtaz KA, Erasenthiran P, Hopkinson N. High density selective

laser melting of Waspaloy®. Journal of Materials Processing Technology. 2008;195:77-87.

11 Sailer I, Makarov NA, Thoma DS, Zwahlen M, Pjetursson BE. All-ceramic or metal-ceramic tooth-supported fixed dental prostheses (FDPs)? A systematic review of the survival and complication rates. Part I: single crowns (SCs). Dental Materials. 2015;31:603-23.

12 Zeng L, Xiang N, Wei B. A comparison of corrosion resistance of cobalt-chromium-molybdenum metal ceramic alloy fabricated with selective laser melting and traditional processing. The Journal of Prosthetic Dentistry. 2014;112:1217-24.

13 ISO 9693-1:2012 Dentistry-Compatibility Testing-Part 1: Metal-Ceramic Systems; International Organization for Standardization: Geneva, Switzerland, 2012.

14 Mehulić K, Lauš-Šošić M. Metal-ceramic bond: how to improve? Minerva Stomatologica. 2009;58:367.

15 Tabernero I, Lamikiz A, Martínez S, Ukar E, De Lacalle LL. Modelling of energy attenuation due to powder flow-laser beam interaction during laser cladding process. Journal of Materials Processing Technology. 2012;212:516-22.

16 Dixit U, Joshi S, Davim JP, Design. Incorporation of material behavior in modeling of metal forming and machining processes: A review. Materials. 2011;32:3655-70.

17 Silva CA, Rosa P, Martins P. Innovative testing machines and methodologies for the mechanical characterization of materials. Experimental Techniques. 2016;40:569-81.

18 Krahmer DM, Polvorosa R, De Lacalle LL, Alonso-Pinillos U, Abate G, Riu F. Alternatives for specimen manufacturing in tensile testing of steel plates. Experimental Techniques. 2016;40:1555-65.

19 ISO 22674:2016 Dentistry-Metallic materials for fixed and removable restorations and appliances; International Organization for Standardization: Geneva, Switzerland, 2016.

20 Zhou Y, Li N, Yan J, Zeng Q. Comparative analysis of the microstructures and mechanical properties of Co-Cr dental alloys fabricated by different methods. The Journal of Prosthetic Dentistry. 2018;120:617-23.

21 Kim HR, Jang S-H, Kim YK, Son JS, Min BK, Kim K-H et al. Microstructures and mechanical properties of Co-Cr dental alloys fabricated by three CAD/CAM-based processing techniques. Materials. 2016;9:596.

22 Al Jabbari Y, Koutsoukis T, Barmpagadaki X, Zinelis S. Metallurgical and interfacial characterization of PFM Co - Cr dental alloys fabricated via casting, milling or selective laser melting. Dental Materials. 2014;30:e79-e88.

23 Øilo M, Nesse H, Lundberg OJ, Gjerdet NR. Mechanical properties of cobalt-chromium 3-unit fixed dental prostheses fabricated by casting, milling, and additive manufacturing. The Journal of Prosthetic Dentistry. 2018;120:156.

24 Takaichi A, Kajima Y, Kittikundecha N, Htat HL, Cho HHW, Hanawa T et al. Effect of heat treatment on the anisotropic microstructural and mechanical properties of Co - Cr - Mo alloys produced by selective laser melting. Journal of the Mechanical

Behavior of Biomedical Materials. 2020;102:103496.

25 Lu Y, Gan Y, Lin J, Guo S, Wu S, Lin J. Effect of laser speeds on the mechanical property and corrosion resistance of CoCrW alloy fabricated by SLM. Rapid Prototyping Journal. 2017.

26 Yan X, Xu Y-X, Wu Y, Lin H. Effects of heat treatment on metal-ceramic combination of selective laser melted cobalt chromium alloy. The Journal of Prosthetic Dentistry. 2018;120:319.

27 Yan X, Lin H, Wu Y, Bai W. Effect of two heat treatments on mechanical properties of selective laser melted Co-Cr metal ceramic alloys for application in thin removable partial dentures. The Journal of Prosthetic Dentistry. 2018;119:1028.

28 Wang H, Feng Q, Li N, Xu S. Evaluation of metal-ceramic bond characteristics of three dental Co-Cr alloys prepared with different fabrication techniques. The Journal of Prosthetic Dentistry. 2016;116:916-23.

29 Kaleli N, Saraç D. Comparison of porcelain bond strength of different metal frameworks prepared by using conventional and recently introduced fabrication methods. The Journal of Prosthetic Dentistry. 2017;118:76-82.

30 Li J, Chen C, Liao J, Liu L, Ye X, Lin S et al. Bond strengths of porcelain to cobalt-chromium alloys made by casting, milling, and selective laser melting. The Journal of Prosthetic Dentistry. 2017;118:69-75.

31 Wul Z. Evaluation of the mechanical properties and porcelain bond strength of cobalt-chromium dental alloy fabricated by selective laser melting. The Journal of Prosthetic Dentistry. 2014;111:51-5.

32 Han X, Sawada T, Schille C, Schweizer E, Scheideler L, Geis-Gerstorfer J et al. Comparative analysis of mechanical properties and metal-ceramic bond strength of Co-Cr dental alloy fabricated by different manufacturing processes. Materials. 2018;11:1801.

33 Howe J. Bonding, structure, and properties of metal/ceramic interfaces: part 1 chemical bonding, chemical reaction, and interfacial structure. International Materials Reviews. 1993;38:233-56.

34 Xin X, Chen J, Xiang N, Gong Y, Wei B. Surface characteristics and corrosion properties of selective laser melted Co‐Cr dental alloy after porcelain firing. Dental Materials. 2014;30:263-70.

35 Reyes M, Oshida Y, Andres C, Barco T, Hovijitra S, Brown D. Titanium‐porcelain system. Part III: effects of surface modification on bond strengths. Bio-medical Materials Engineering 2001;11:117-36.

36 Maressa P, Anodio L, Bernasconi A, Demir AG, Previtali B. Effect of surface texture on the adhesion performance of laser treated Ti6Al4V alloy. The Journal of Adhesion. 2015;91:518-37.

37 Xiang N, Xin X-Z, Chen J, Wei B. Metal‐ceramic bond strength of Co‐Cr alloy fabricated by selective laser melting. Journal of Dentistry. 2012;40:453-7.

38 Xin X-Z, Xiang N, Chen J, Xu D, Wei B. Corrosion characteristics of a selective laser melted Co‐Cr dental alloy under physiological conditions. Journal of Materials Science. 2012;47:4813-20.

39 Dimitriadis K, Papadopoulos T, Agathopoulos S. Effect of Bonding

Agent on Metal Ceramic Bond Strength between Co Cr Fabricated with Selective Laser Melting and Dental Feldspathic Porcelain. Journal of Prosthodontics. 2019;28:1029-36.

40 Al Bakkar H, Spintzyk S, Schille C, Schweizer E, Geis-Gerstorfer J, Rupp F. Influence of a bonding agent on the bond strength between a dental Co-Cr alloy and nine different veneering porcelains. Biomedical Engineering/Biomedizinische Technik. 2016;61:509-17.

41 Park WU, Park HG, Hwang KH, Zhao J, Lee JK. Interfacial property of dental cobalt-chromium alloys and their bonding strength with porcelains. Journal of Nanoscience and Nanotechnology. 2017;17:2585.

42 Külünk T, Kurt M, Ural Ç, Külünk Ş, Baba S. Effect of different air-abrasion particles on metal-ceramic bond strength. Journal of Dental Sciences. 2011;6:140-6.

-국문초록-

선택적 레이저 용융 방식으로 제작한 코발트-크롬 합금의 금속-세라믹 결합강도와 기계적인 성질

서울대학교 대학원 치의과학과 치과보철학 전공
(지도교수 김 성 균)
홍 준 기

목 적: 적층 가공 기술의 발달과 제작 방식의 장점으로 인해 치과 영역에 3D 프린팅 기술의 적용 범위가 늘어가고 있다. 하지만 3D 프린팅과 기존의 방식으로 제작한 보철물의 여러 특성을 비교한 연구가 부족하다. 본 연구의 목적은 3D 프린팅 방식의 한 종류인 선택적 레이저 용융(Selective Laser Melting; SLM) 방식으로 제작한 코발트-크롬 합금의 기계적인 성질과 세라믹과의 결합강도가 기존의 주조, 절삭가공 방식으로 제작한 합금과 차이가 있는지 알아보는 것이다.

재료 및 방법: 먼저 합금의 기계적인 성질을 측정하기 위해서 주괴(Star Loy C, Dentsply Sirona, Pennsylvania, USA)를 이용한 주조, 디스크(Starbond Co-Cr block, Scheftner dental alloys, Mainz, Germany)를 이용한 밀링, 파우더(SP2, EOS, Krailling, Germany)를 이용한 SLM 3가지 다른 방식으로 코발트-크롬 합금을 제작하였다. ISO 22674:2016 규격에 따라 34 × 13 × 1.5 mm 크기의 판 모양으로 시편을 제작했다. 각 그룹별로 12개의 시편을 준비해 3점 굽힘 실험을 통해 금속의 응력-

변형 곡선을 그리고, 탄성계수, 항복강도, 굴곡강도를 계산했다. 또한, 금속 - 세라믹의 결합강도 측정을 위해 ISO 9693-1:2012 규격에 따라 시편을 똑같이 세 가지 방법으로 25 × 3 × 0.5 mm 크기로 제작하고, 그 위의 중앙 부위에 세라믹(Hera Ceram, Heraeus, Hanau, Germany)을 8 × 3 × 1.1 mm 크기로 올린 시편을 각 12개씩 제작했다. 이후에 3점 굽힘 실험을 통해 금속-세라믹 결합 강도(τ_b)를 측정했다. 실험 후 각 실험군 당 5개의 시편을 무작위로 추출해 시편 당 3개 부위에서 표면의 미세거칠기(R_a)를 측정하고, 세라믹이 탈락한 표면의 성분분석을 진행했다. 또한 주사전자현미경을 이용해 금속의 표면을 관찰했다. 통계적 분석은 각 실험 결과를 Levene's test를 통해 등분산 확인하고, 3가지의 다른 제작 방법에 대하여 미세거칠기, 탄성계수, 항복강도, 굴곡강도, 결합강도, 금속 표면에 세라믹이 남아있는 비율을 종속변수로 일원 분산 분석 시행하고, Tukey's post-hoc test로 사후 검정했다 (α = 0.05).

결 과: 미세거칠기는 각 실험군 사이에 통계적인 차이는 없는 것으로 나타났다. (주조군 1.19 ± 0.58 μm, 밀링군 0.88 ± 0.46 μm, SLM군 1.10 ± 0.30 μm) 탄성계수는 주조군에서 더 크게 나타났다. (주조군 560.53 ± 21.53 GPa, 밀링군 473.55 ± 35.02 GPa, SLM군 464.55 ± 10.77 GPa) 항복강도와 (주조군 567.92 ± 35.53 MPa, 밀링군 323.86 ± 32.04 MPa, SLM군 591.18 ± 22.31 MPa) 굴곡강도는 (주조군 792.31 ± 81.64 MPa, 밀링군 494.16 ± 51.93 MPa, SLM군 849.48 ± 24.45 MPa) 밀링군에서 작게 나타났다. 금속의 파절면을 주사전자현미경으로 관찰한 결과, 주조군에서는 주조 후에 불균일하게 식으면서 생기는 특징적인 수지상 구조를 관찰할 수 있었고, 밀링군에서는 균일한 표면을 볼 수 있었다. SLM군에서는 나노크기의 결정구조를 볼 수 있었다. 밀링군에서는 파절면에서 물결무늬를 관찰할 수 있었고, SLM군에서는 계단면처럼 보이는 파절 양상을 볼 수 있었다. 금속-세라믹 결합강도(τ_b)를 측정한 결과, 주조군

이 높게 나왔다. (주조군 32.51 ± 2.68 MPa, 밀링군 26.98 ± 3.97 MPa, SLM군 29.07 ± 2.90 MPa) 하지만 ISO 규격에 따르면 세 군 모두 기준치를 만족하는 결과를 보였다. 세라믹이 탈락한 면을 보면 금속 표면에 세라믹이 남아있는 것을 관찰할 수 있었다. 성분분석(EDS) 결과 표면에서 규소가 검출된 비율이 밀링군, SLM군, 주조군의 순서로 나타났으며, (주조군 36.44 ± 6.37 %, 밀링군 57.10 ± 12.26 %, SLM군 49.50 ± 7.69 %) 모두 혼합된 탈락양상을 보였다.

결 론: 세 가지 다른 방법으로 제작한 코발트 - 크롬 합금의 미세거칠기 값은 통계적으로 차이가 없었다. 기계적인 성질 중에서 탄성계수는 주조군이 높았고, 항복강도와 굴곡강도는 밀링군이 낮았다. 세라믹 탈락면을 검사하면, 모두 혼합된 탈락양상을 보였다. 주조, 밀링, SLM 제작 방식에 따라 결과의 차이는 있었지만, ISO 기준에 따르면 세 군 모두 결합강도가 임상적으로 사용 가능한 기준을 통과한 것으로 나타났다. 여러 특성을 고려했을 때, 선택적 레이저 용융 방식은 기존의 전통적인 제작방법을 대체할 가능성이 있을 것으로 보인다.

주요어: 3D 프린팅; selective laser melting; 코발트 - 크롬 합금; 금속 - 세라믹 결합강도; 3점 굽힘 실험

학 번: 2017-36370